ISSN 0023-1584, Kinetics and Catalysis, 2008, Vol. 49, No. 1, pp. 18–26. © MAIK "Nauka/Interperiodica" (Russia), 2008.
Original Russian Text © I.A. Kotareva, I.V. Oshanina, K.Yu. Odintsov, L.G. Bruk, O.N. Temkin, 2008, published in Kinetika i Kataliz, 2008, Vol. 49, No. 1, pp. 22–30.

Kinetics and Mechanism of Carbon Monoxide Oxidation on the Supported Metal Complex Catalyst $PdCl_2$–$CuCl_2/Al_2O_3$

I. A. Kotareva, I. V. Oshanina, K. Yu. Odintsov, L. G. Bruk, and O. N. Temkin

Lomonosov State Academy of Fine Chemical Technology, Moscow, 119571 Russia

e-mail: lbruk@rol.ru

Received June 9, 2007

Abstract—The kinetics of carbon monoxide oxidation with atmospheric oxygen on a $PdCl_2$–$CuCl_2/\gamma$-Al_2O_3 catalyst was studied at T = 27°C and an N_2–O_2–CO mixture pressure of 1 atm. The catalyst was prepared by cold impregnation. Three groups of mechanistic hypotheses are considered, and two of them are demonstrated to be consistent with kinetic data, although they differ in the roles of water and oxygen in carbon monoxide oxidation.

DOI: 10.1134/S0023158408010035

The oxidation of carbon monoxide, which is among the most common and best understood reactions, is carried out using both homogeneous and heterogeneous catalysts [1–3]. The most frequent components of homogeneous catalytic systems are palladium halides and oxidizing cocatalysts, such as copper(II) and iron(III) compounds, quinones, and heteropoly acids [1–5]. The most usual commercial oxidizer is air. It has recently been demonstrated that, when the reaction is conducted in a 1,4-dioxane or THF solution of palladium bromide, molecular oxygen is a sufficiently efficient oxidizer and requires no cocatalyst [6]. However, the most efficient catalytic systems for CO oxidation involve the above cocatalysts. The widest use in this reaction has been gained by heterogeneous catalysts, which are conventionally divided into metallic, oxide, metal complex, and mixed catalysts [5].

The least attention has been given to CO oxidation involving metal complexes and mixed catalysts. This is likely due to the lack of necessary information concerning the state of active components on the support surface. The mechanism of CO oxidation on supported metal complex catalysts involving Pd(II) and Cu(II) compounds [7–13] has been analyzed in terms of catalysis with liquid-phase supported catalysts. The rate of CO oxidation in the CO + O_2 + N_2 mixture on $PdCl_2$–$CuCl_2/Al_2O_3$ catalysts at T = 333 K and atmospheric pressure was observed to be proportional to the palladium(II) chloride content to the first power and to the copper(II) chloride content to a power of 0–1 [10]. The CO oxidation rate equation was found to be of the order of –0.5 with respect to oxygen and of the order of 1.0 with respect to carbon monoxide. It was demonstrated that water vapor plays a significant role in the reaction system. The authors of those studies provided no satisfactory explanation for their observations.

In a series of works [7–9], the kinetics of this reaction at 25°C was studied in the presence of supported $PdCl_2$–$CuCl_2$ catalysts containing an alkali-metal chloride or bromide. The reaction rate was proportional to the palladium salt content and depended in a complicated way on the $CuCl_2$ content and on the water concentration in the catalyst. The orders of the reaction with respect to the partial pressures of carbon monoxide and oxygen were not determined.

There have been in situ IR spectroscopic studies of the state of the active components of alumina- and activated carbon–supported $PdCl_2$–$CuCl_2$ catalysts in contact with CO, O_2, and water vapor [11–13]. These studies revealed the formation of the carbonyls $PdCl_2(CO)$, $[Pd(CO)Cl]_n$, and Cu(CO)Cl and minor amounts of terminal and bridging CO groups bonded to palladium metal particles. The activity of the catalysts in CO oxidation was higher by 1–3 orders of magnitude in the presence of water vapor [12]. The kinetics of CO oxidation over these catalysts was studied at 300–450 K and comparatively high partial pressures of CO (up to 0.13 atm) and O_2 (up to 0.25 atm). The order of the reaction with respect to P_{CO} varied between 0 and –1, and the order of the reaction with respect to P_{O_2} increased from 0.2 to 0.7 at pressures above 0.07 atm [13].

The kinetics of the reaction at low temperatures (300–400 K) was explained in terms of a model assuming that adsorbed CO and O_2 react along the perimeters of "islands" resulting from the adsorption of these molecules on the surface of the catalyst. At higher temperatures, the reaction can adequately be described using the Langmuir–Hinshelwood model [13].

The state of the active components of $PdCl_2$–$CuCl_2$/activated carbon and $PdCl_2$–$CuCl_2/Al_2O_3$ catalysts was also studied by X-ray diffraction and X-ray spectroscopy [14–17]. Furthermore, Park and Lee [17] used temperature-programmed desorption and IR spectroscopy. The results of those studies provide the following findings: most of the copper is in the form of the crystalline phase $Cu_2Cl(OH)_3$, the CO oxidation activity of the catalyst is correlated with the amount of this phase, and the most likely state of palladium in the active form of the catalyst is Pd(II) in the chloride ligand environment. Furthermore, the results obtained allow the presence of carbonyl ligands in the coordination sphere of palladium(II) in the solid phase.

Depending on process conditions (temperature and the $CO : O_2 : H_2O$ ratios), part of the palladium and copper may be reduced to Pd(I) or Pd(0) and Cu(I), respectively. According to the data obtained for homogeneous systems based on palladium complexes, Pd(I) complexes are more active than Pd(II) compounds. No such data are available for the corresponding supported catalysts.

The authors of the above-quoted works believe that water plays a dual role. In the framework of the liquid-phase supported catalyst model, it serves as a solvent for the active components of the catalyst. The rate of the process is much higher in the presence of water vapor. At the same time, raising the relative humidity to 100% slows down the process dramatically [17]. Similar data were obtained in an earlier study [7], and this suggests that water can act as a catalyst: it may participate in CO_2 formation steps and may be regenerated via the interaction between oxygen and the reduced forms of the catalyst, as in the mechanisms proved for homogeneous systems [2, 4]. The deactivation of the catalyst at high water concentrations is due to the formation of the palladium metal phase.

None of the above-quoted work presents a mechanism that could provide a quantitative description for the effect of the CO, O_2, and H_2O partial pressures on the carbon dioxide formation rate.

Here, we report the kinetics and the chosen mechanism of carbon monoxide oxidation with atmospheric oxygen over a $PdCl_2$–$CuCl_2/\gamma$-Al_2O_3 catalyst under mild conditions ($N_2 + O_2 + CO$ mixture, atmospheric pressure, 27°C). In the absence of palladium, the catalyst is inactive under these conditions.

EXPERIMENTAL

Kinetics were studied in a temperature-controlled glass flow reactor having a catalyst shelf and a well for an electronic thermometer. The reactor was charged with 1.7 ml (0.8 g) of a $PdCl_2$–$CuCl_2/Al_2O_3$ catalyst containing 0.4 wt % Pd and 5 wt % Cu (bed height of 4 mm). The catalyst was prepared by cold impregnation [22, 23] as 30- to 50-ml batches. The reproducibility of the properties of the catalyst was checked by special-purpose experiments. Each kinetic run was performed with a fresh portion of the catalyst. The initial nitrogen–oxygen–carbon monoxide gas mixture was prepared by mixing an air stream from a compressor (or a nitrogen stream from a cylinder) with a stream of carbon monoxide (if necessary, mixed with air, nitrogen, or oxygen) from a gasometer.

The partial pressure of water in the feed was controlled by passing part of the air stream through a humidifier or through a drier (molecular sieve). In experiments at a preset gas humidity φ, the catalyst in the reactor was pretreated with air of the same humidity until the establishment of a steady state (until the inlet and outlet φ values were equal) in order to ensure that the water content of the catalyst surface is constant during the run.

The reactor temperature was measured with an electronic thermometer, whose sensor was placed in the catalyst bed. Gas flows were monitored using calibrated differential pressure flowmeters. The air (or nitrogen) feed rate before the run and the gas mixture flow rate at the outlet of the reactor were measured with a GSB-400 gas meter. The inlet and outlet water contents of the gas were measured using IVTM-7 humidity meters with electrochemical sensors. The gas composition was determined by gas chromatography. Oxygen, nitrogen, and CO were separated in a 3-m-long column packed with the molecular sieve 13X (0.25–0.5 mm size fraction). The column temperature was 40°C, the components were detected with a thermal-conductivity detector, and the carrier gas was argon. Carbon dioxide was determined using a 3-m-long column packed with activated carbon AR-3 (separation temperature of 160°C, thermal-conductivity detector, argon as the carrier gas). The experimental setup is schematized in Fig. 1.

All runs were carried out at O_2 and CO conversions no higher than 15%, so that it was possible to consider the reactor to be differential. The CO_2 formation rate was derived from the gas outflow rate and the composition (CO_2 content) data. No CO_2 was detected in the feed. Kinetic data were processed using the O_2, H_2O, and CO partial pressures at the reactor outlet.

Kinetic data processing was based on models corresponding to different hypothetical mechanisms. The numerical values of rate constants were estimated using a program realizing the coordinate descent method. Since the resulting estimates were possibly dependent on the initial approximation (the initial values of the constants) and on the functional minimum search interval (the residual sum of the squared differences between the calculated and observed reaction rates), the initial values of the constants were varied in a wide range. The model validity criteria were the residual sum of squared deviations and the visually estimated degree of coincidence between the observed and calculated

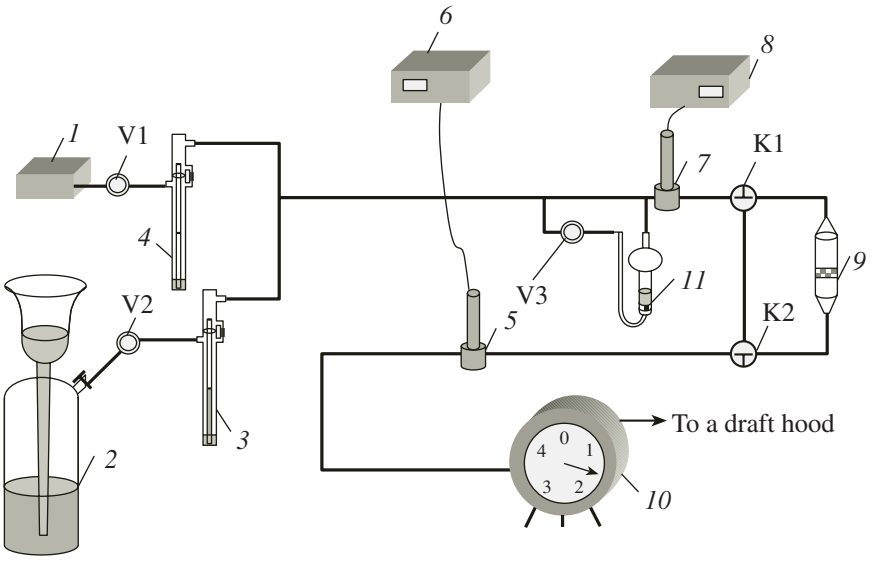

Fig. 1. Schematic of the catalytic activity measurement setup: (*1*) compressor, (*2*) gasometer, (*3*, *4*) differential pressure flowmeters, (*5* + *6*, *7* + *8*) humidity meters with their sensors, (*9*) reactor, (*10*) gas meter; (*11*) saturator; (V1, V2, V3) needle valves, (K1, K2) three-way valves.

partial dependences of the reaction rate on the O_2, H_2O, and CO partial pressures.

RESULTS AND DISCUSSION

Hypothetical Mechanisms of CO Oxidation

The literature data discussed above suggest that an active site of the catalyst contains palladium and copper in their oxidized (Pd(II), Cu(II)) or reduced (Pd(I), Cu(I)) states. In the first approximation, the process can be considered to occur on palladium- and copper-containing active sites of one type. The possible mechanisms are divided into three groups (A, B, and C) according to the role played by water and molecular oxygen.

Hypothesis group A consists of mechanisms in which carbon dioxide results from the interaction between CO and H_2O on an active site of the catalyst (Z):

$$\begin{aligned} Z + CO + H_2O &\longrightarrow CO_2 + Z(H)_2, \\ 2Z(H)_2 + O_2 &\longrightarrow 2H_2O + 2Z. \end{aligned} \qquad \text{(I)}$$

The function of oxygen in the group A mechanisms is to oxidize the reduced forms of the metals of the active site or the hydrides bound to this site. The group A mechanisms are similar to the well-known mechanism of ethylene oxidation into acetaldehyde [18].

Hypothesis group B consists of mechanisms in which carbon dioxide results directly from oxygen and CO on an active site of the catalyst:

$$\begin{aligned} Z + CO + O_2 &\longrightarrow ZO + CO_2, \\ ZO + CO &\longrightarrow Z + CO_2. \end{aligned} \qquad \text{(II)}$$

In the group B mechanisms, water does not participate in the formation of CO_2. These mechanisms can be realized not only on metal and oxide catalysts [19, 20], but also in homogeneous metal complex systems [21].

The **group C mechanisms** assume that both water and oxygen are involved in carbon dioxide formation. This can take place, for example, as follows:

$$\begin{aligned} Z + CO + H_2O &\longrightarrow Z(H)_2 + CO_2, \\ Z(H)_2 + O_2 &\longrightarrow ZO + H_2O, \\ ZO + CO &\longrightarrow Z + CO_2. \end{aligned} \qquad \text{(III)}$$

In this case, the reactions involving water and oxygen yield equal amounts of CO_2. Group C also includes a chain mechanism in which the reduction of Pd(II) and Cu(II) with carbon monoxide to Pd(I) and Cu(I), respectively, generates an active site and this site then catalyzes CO oxidation:

$$\begin{aligned} Z + CO + H_2O &\longrightarrow Z(H)_2 + CO_2, \\ Z(H)_2 + CO &\overset{K_2}{\rightleftharpoons} (CO)Z(H)_2, \\ (CO)Z(H)_2 + O_2 &\longrightarrow (O)Z(H)_2 + CO_2, \\ (O)Z(H)_2 + CO &\longrightarrow Z(H)_2 + CO_2, \\ (O)Z(H)_2 &\longrightarrow Z + H_2O. \end{aligned} \qquad \text{(IV)}$$

Mechanism (IV) (Fig. 2) includes two cycles (two linearly independent routes).

In order to discriminate between different hypotheses and between kinetic models based on them, we studied the kinetics of the process.

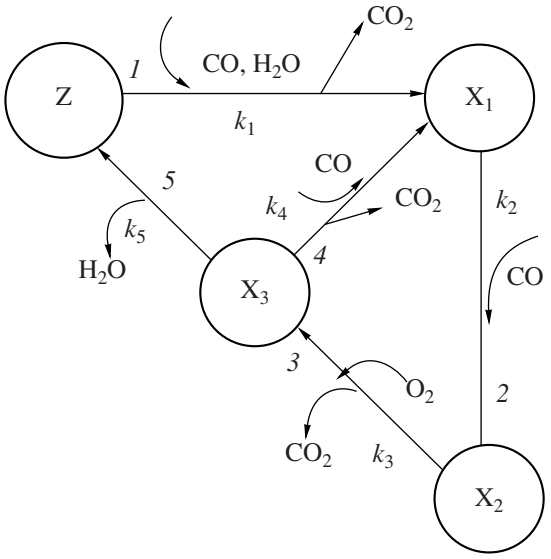

Fig. 2. Graph of mechanism (IV): $X_1 = Z(H)_2$, $X_2 = (CO)Z(H)_2$, and $X_3 = (O)Z(H)_2$.

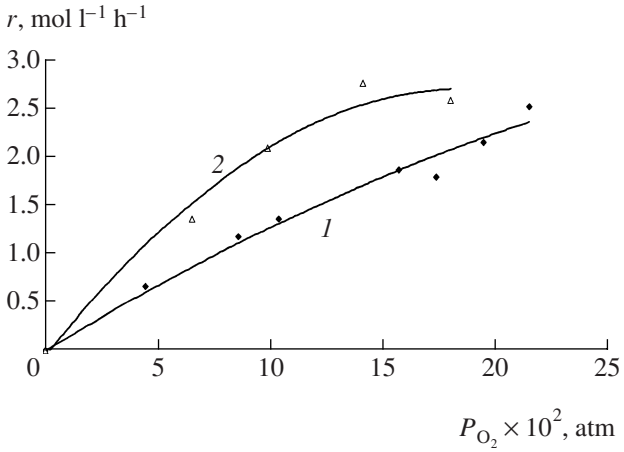

Fig. 3. Carbon dioxide formation rate as a function of the oxygen partial pressure: (*1*) $P_{CO} = 0.05$ atm, $P_{H_2O} = 0.009$ atm, $\varphi = 6$ g/m^3; (*2*) $P_{CO} = 0.05$ atm, $P_{H_2O} = 0.0135\leq$ atm, $\varphi = 10$ g/m^3.

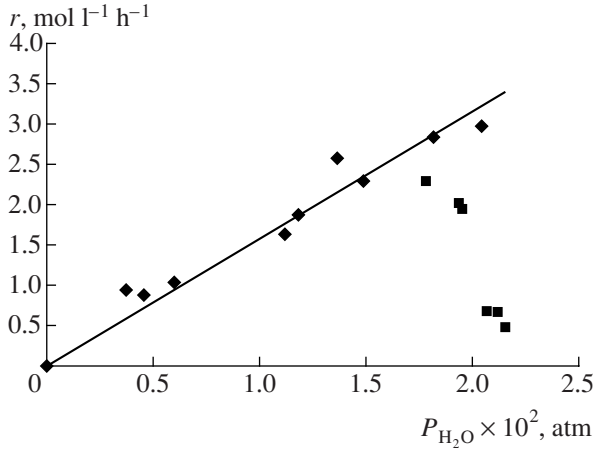

Fig. 4. Carbon dioxide formation rate as a function of the water partial pressure at $P_{O_2} = 0.18$ atm and $P_{CO} = 0.05$ atm.

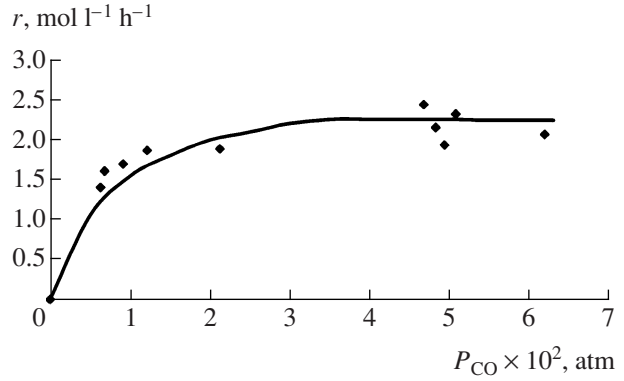

Fig. 5. Carbon dioxide formation rate as a function of the CO partial pressure at $P_{O_2} = 0.18$ atm and $P_{H_2O} = 0.009$ atm ($\varphi = 6$ g/m^3).

Discrimination of Hypotheses

The reaction was conducted under conditions such that the effect of the diffusion factors was ruled out. For this purpose, we initially studied how the CO oxidation rate depends on the catalyst particle size and on the linear gas velocity. We found that kinetic measurements should be made on catalyst samples with a particle size of 0.5–1 mm at a feed flow rate of 21 l/h (~12400 h^{-1}). These conditions ensured a kinetically controlled regime of the reaction and a comparatively low conversion of the reactants.

The dependences of the CO_2 formation rate on the partial pressures of O_2, H_2O, and CO were studied by varying one of these pressures while maintaining the other pressures nearly constant (single-factor experiments). The results of these experiments are presented in Figs. 3–5 and Table 1. The calculation of the CO_2 formation rate using different equations was carried out for parameters nearly constant within each particular series of runs and for given points. Accordingly, the calculated data listed below are discrete, as are the corresponding experimental data.

At a water content of $\varphi = 6$ g/m^3 ($P_{H_2O} = 0.009$ atm), the dependence of the CO_2 formation rate (r) on the oxygen partial pressure is nearly linear. As the water content increases, the observed order of the reaction with respect to oxygen slightly decreases (Fig. 3).

The reaction rate as a function of H_2O partial pressure passes through an extremum and drops down abruptly at $P_{H_2O} \approx 0.02$ atm (Fig. 4). It is likely that the state of the catalyst changes at this pressure. In data processing, we took into consideration only the data points lying below $P_{H_2O} = 0.02$ atm.

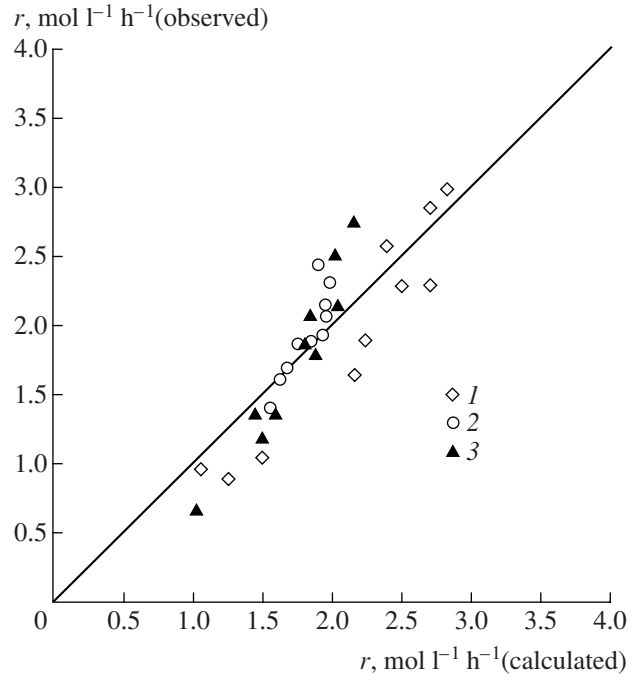

Fig. 6. Results of kinetic data processing using Eq. (2), which corresponds to mechanism (V): (*1*) variation of P_{H_2O} at nearly constant P_{CO} and P_{O_2}, (*2*) variation of P_{CO} at nearly constant P_{H_2O} and P_{O_2}, and (*3*) variation of P_{O_2} at nearly constant P_{CO} and P_{H_2O}.

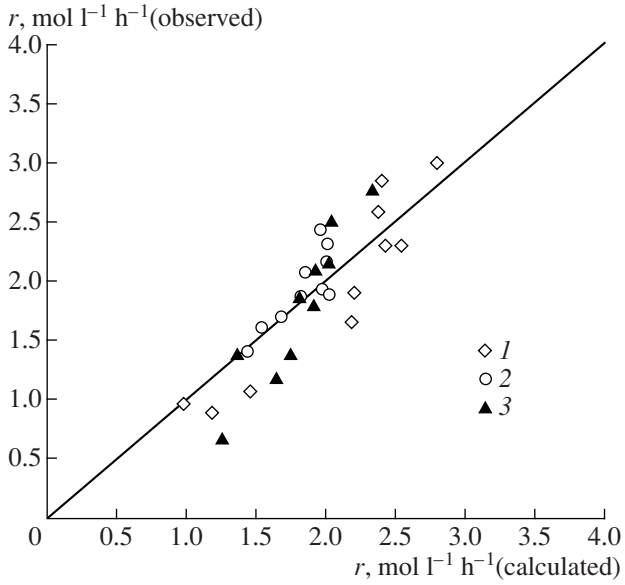

Fig. 7. Results of kinetic data processing using Eq. (3), which corresponds to mechanism (VI): (*1*) variation of P_{H_2O} at nearly constant P_{CO} and P_{O_2}, (*2*) variation of P_{CO} at nearly constant P_{H_2O} and P_{O_2}, and (*3*) variation of P_{O_2} at nearly constant P_{CO} and P_{H_2O}.

The CO_2 formation rate depends very slightly on the CO partial pressure (Fig. 5).

The formal orders of the reaction with respect to O_2, H_2O, and CO ($n_i = \partial \ln r / \partial \ln P_i|_{P_{k,i} = \text{const}}$) in the power-law equation (1) are, respectively, 0.8, 0.6, and 0.2:

$$r = kP_{O_2}^{0.8}P_{H_2O}^{0.6}P_{CO}^{0.2}. \quad (1)$$

These values were used in further analysis to discriminate mechanistic hypotheses. Discrimination was carried out by estimating the constants in the equations corresponding to the above three groups of mechanisms. Each group involves about twenty mechanisms and the corresponding models. Below, we present the simplest group A and C mechanisms and models that provide a reasonably good fit to experimental data.

Group A mechanisms. In the group A mechanisms, oxygen serves to regenerate the active sites of the catalyst. The reaction can have a comparatively large order with respect to oxygen only if the intermediates with which oxygen reacts (mechanisms (V) and (VI)) are involved in surface coverage. Mechanism (V) can be represented as

$$\begin{aligned}
&(1)\ Z + CO \overset{K_1}{\rightleftharpoons} Z(CO),\\
&(2)\ Z + H_2O \overset{K_2}{\rightleftharpoons} Z(H_2O),\\
&(3)\ Z(H_2O) + CO \overset{K_3}{\rightleftharpoons} Z(H_2O)(CO),\\
&(4)\ Z(H_2O)(CO) \longrightarrow Z(H)_2 + CO_2,\\
&(5)\ Z(H)_2 + O_2 \longrightarrow HZ(OOH),\\
&(6)\ HZ(OOH) \longrightarrow Z + H_2O_2,\\
&(7)\ 2H_2O_2 \longrightarrow 2H_2O + O_2.
\end{aligned} \quad (V)$$

The following CO_2 formation rate equation corresponds to this scheme:

$$r = \frac{k_1P_{CO}P_{O_2}P_{H_2O}}{P_{O_2} + k_2P_{CO}P_{O_2} + k_3P_{O_2}P_{H_2O} + k_4P_{CO}P_{H_2O} + k_5P_{CO}P_{O_2}P_{H_2O}}. \quad (2)$$

Equation (2), like the equations presented below, involves apparent, or effective, constants that are complicated functions of the rate constants and equilibrium constants of the elementary steps included in the hypothetical mechanisms.

The surface coverage balance in mechanism (V)

takes into consideration the intermediates Z, Z(CO), $Z(H_2O)$, $Z(H_2O)(CO)$, and $Z(H)_2$ (the surface area fraction occupied by $Z(H)_2$ was derived from the quasi-stationarity condition for this intermediate).

Mechanism (VI) appears as follows:

$$\begin{aligned}
&(1)\ Z + CO \overset{K_1}{\rightleftarrows} Z(CO),\\
&(2)\ Z(CO) + H_2O \overset{K_2}{\rightleftarrows} Z(H_2O)(CO),\\
&(3)\ Z(H_2O)(CO) \xrightarrow{k_3'} Z(H)_2 + CO_2, \qquad \text{(VI)}\\
&(4)\ 2Z + O_2 \overset{K_4}{\rightleftarrows} 2ZO,\\
&(5)\ ZO + Z(H)_2 \longrightarrow 2Z + H_2O.
\end{aligned}$$

The corresponding surface coverage balance takes into account the intermediates Z, Z(CO), $Z(H_2O)(CO)$, $Z(H)_2$, and ZO (the surface area fraction occupied by $Z(H)_2$ derived from the quasi-stationarity condition, $\theta_{Z(H)_2} = \dfrac{k_3'K_1K_2P_{CO}P_{H_2O}}{K_4^{0.5}P_{O_2}^{0.5}}$, is independent of θ_Z).

The following rate equation corresponds to mechanism (VI):

$$r = \frac{k_1P_{CO}P_{O_2}^{0.5}P_{H_2O} - k_2P_{CO}^2P_{H_2O}^2}{P_{O_2}^{0.5}(1 + k_3P_{CO} + k_4P_{CO}P_{H_2O} + k_5P_{O_2}^{0.5})}. \qquad (3)$$

On the whole, Eqs. (2) and (3) provide a good fit to experimental data (Figs. 6, 7).

A drawback of the above models is that they do not provide a sufficiently good fit to the observed partial dependence of the CO_2 formation rate on the oxygen partial pressure. At low P_{O_2} values, the calculated r values deviate systematically from the experimental r data (see the data points for $\varphi = 6$ g/m^3 in Figs. 8 and 9).

The observed strong effect of P_{H_2O} on the carbon dioxide formation rate (formal reaction order of 0.6) allows the group B mechanisms, which do not involve water, to be left out of consideration.

The group C mechanisms, in which water and oxygen are directly involved in CO_2 formation, seem to be the most likely.

Group C mechanisms. Below, we present the simplest variant of the group C mechanisms, which includes carbon monoxide and water adsorption on the active site followed by an attack of oxygen from the gas phase:

$$\begin{aligned}
&(1)\ Z + CO \overset{K_1}{\rightleftarrows} Z(CO),\\
&(2)\ Z(CO) + H_2O \overset{K_2}{\rightleftarrows} Z(H_2O)(CO),\\
&(3)\ Z(H_2O)(CO) + O_2 \longrightarrow CO_2 + ZO + H_2O, \qquad \text{(VII)}\\
&(4)\ ZO + CO \longrightarrow Z + CO_2.
\end{aligned}$$

Table 1. Experimental kinetic data

$P_{CO} \times 10^2$, atm	$P_{O_2} \times 10^2$, atm	$P_{H_2O} \times 10^2$, atm	r, mol l^{-1} h^{-1}
5.46	18.62	0.37	0.953
5.46	18.69	0.46	0.880
5.42	18.27	0.60	1.049
5.16	17.96	1.12	1.633
5.33	17.85	1.19	1.888
5.07	18.00	1.37	2.577
5.09	18.03	1.50	2.282
4.85	18.26	1.79	2.288
5.05	17.86	1.82	2.844
4.32	18.01	2.05	2.985
4.94	18.34	0.90	1.933
4.68	18.24	0.88	2.433
4.83	18.39	0.92	2.151
5.08	18.30	0.94	2.314
2.12	19.11	0.89	1.884
1.21	19.23	0.91	1.863
6.19	18.03	0.92	2.068
0.68	19.52	0.96	1.603
0.63	18.73	0.92	1.397
0.91	18.86	0.92	1.690
5.04	4.45	0.90	0.662
5.23	8.56	0.95	1.172
5.13	10.36	0.91	1.361
5.10	17.37	0.88	1.786
5.38	19.47	0.96	2.140
4.72	21.50	0.91	2.508
5.40	15.71	0.85	1.858
4.82	9.89	1.36	2.082
5.07	6.50	1.29	1.360
4.59	14.12	1.35	2.753

Table 2. Rate constants (k_i) and the residual sums of squared deviations (SS) for different kinetic equations

Equation no.	k_1	k_2	k_3	k_4	k_5	k_6	k_7	SS
(2)	2.4×10^5 mol/(l h atm^2)	6.3×10^2 atm^{-1}	1.3×10^2 atm^{-1}	6.4×10^3 atm^{-1}	1.5×10^4 atm^{-2}	–	–	2.51
(3)	4.5×10^4 mol/(l h atm^2)	1.1×10^7 mol/(l h atm$^{3.5}$)	1.3×10^2 atm^{-1}	7.7×10^{-2} atm^{-2}	4.6×10^{-5} atm$^{-0.5}$	–	–	2.53
(4)	4.0×10^5 mol/(l h atm^3)	2.0×10^2 atm^{-1}	1.3×10^4 atm^{-2}	–	–	–	–	3.41
(5)	5.0×10^5 mol/(l h atm^3)	2.2×10^2 atm^{-1}	1.0×10^{-1} atm^{-2}	1.1×10^5 atm^{-3}	–	–	–	2.28
(6)	2.0×10^4 mol/(l h atm^2)	3.3×10^{-5} atm^{-1}	1.6×10^{-2} (dimensionless)	3.6×10^{-1} atm^{-1}	5.9×10^{-7} atm^{-1}	2.8×10^3 atm^{-2}	1.6×10^4 atm^{-2}	4.56

This mechanism implies the following CO_2 formation rate equation:

$$r = \frac{k_1 P_{CO} P_{O_2} P_{H_2O}}{1 + k_2 P_{CO} + k_3 P_{CO} P_{H_2O}}. \quad (4)$$

This equation provides a satisfactory fit to experimental data (Fig. 10). This variant of the mechanism better accounts for the dependence of the reaction rate on P_{O_2} (Fig. 11), but it does not make clear the function of water.

Below, we present a somewhat more complicated variant that includes the formation of the intermediate $Z(CO)(H_2O)(O_2)$ on the catalyst surface and provides a better fit to experimental data (Figs. 12, 13):

(1) $Z + CO \overset{K_1}{\rightleftharpoons} Z(CO)$,

(2) $Z(CO) + H_2O \overset{K_2}{\rightleftharpoons} Z(H_2O)(CO)$,

(3) $Z(H_2O)(CO) + O_2 \overset{K_3}{\rightleftharpoons} Z(H_2O)(CO)(O_2)$, (VIII)

(4) $Z(H_2O)(CO)(O_2) \longrightarrow CO_2 + ZO(H_2O)$,

(5) $ZO(H_2O) + CO \longrightarrow Z + CO_2 + H_2O$.

The following equation corresponds to this variant:

$$r = \frac{k_1 P_{CO} P_{O_2} P_{H_2O}}{1 + k_2 P_{CO} + k_3 P_{CO} P_{H_2O} + k_4 P_{CO} P_{O_2} P_{H_2O}}. \quad (5)$$

A possible role of water is that its polarized molecule or a hydroxyl ligand attacks coordinated carbon

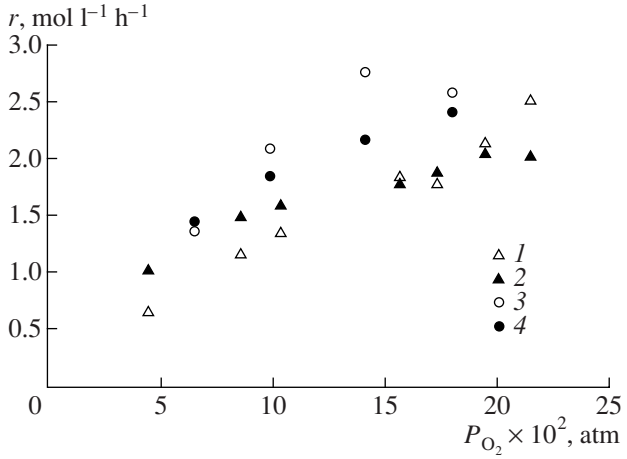

Fig. 8. (*1*, *3*) Observed and (*2*, *4*) calculated dependences of the carbon dioxide formation rate on the oxygen partial pressure at φ = (*1*, *2*) 6 and (*3*, *4*) 10 g/m^3 (calculation using Eq. (2)).

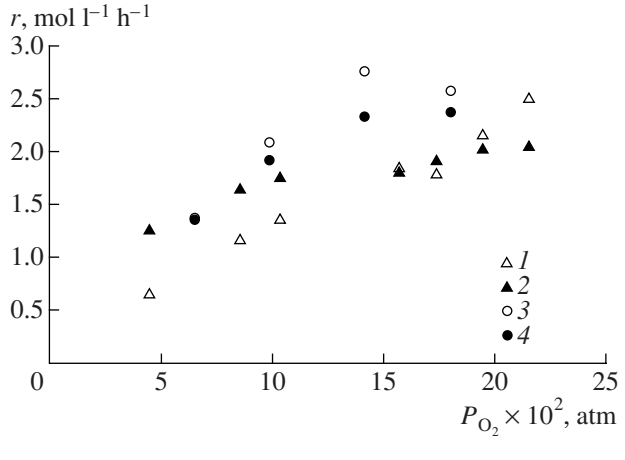

Fig. 9. (*1*, *3*) Observed and (*2*, *4*) calculated dependences of the carbon dioxide formation rate on the oxygen partial pressure at φ = (*1*, *2*) 6 and (*3*, *4*) 10 g/m^3 (calculation using Eq. (3)).

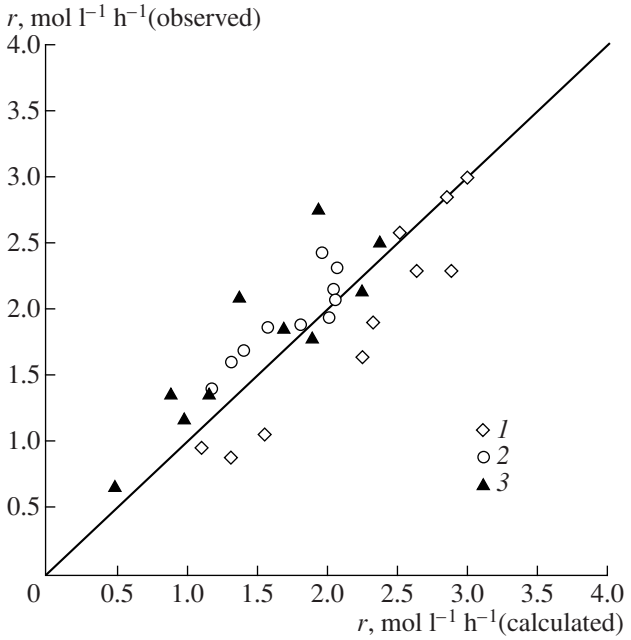

Fig. 10. Results of kinetic data processing using Eq. (4), which corresponds to mechanism (VII): (*1*) variation of P_{H_2O} at nearly constant P_{CO} and P_{O_2}, (*2*) variation of P_{CO} at nearly constant P_{H_2O} and P_{O_2}, and (*3*) variation of P_{O_2} at nearly constant P_{CO} and P_{H_2O}.

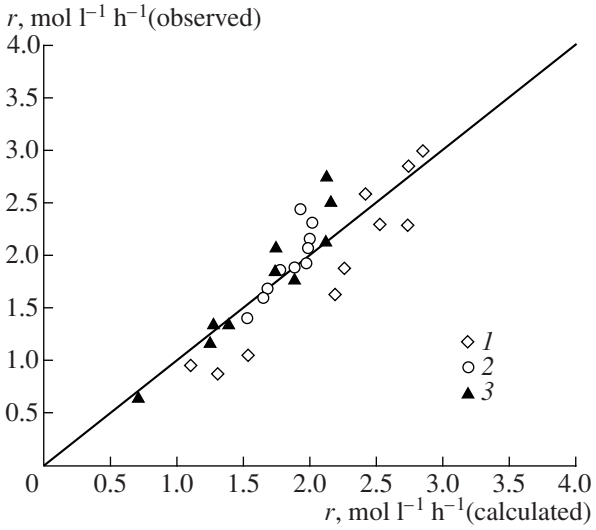

Fig. 12. Results of kinetic data processing using Eq. (5), which corresponds to mechanism (VIII): (*1*) variation of P_{H_2O} at nearly constant P_{CO} and P_{O_2}, (*2*) variation of P_{CO} at nearly constant P_{H_2O} and P_{O_2}, and (*3*) variation of P_{O_2} at nearly constant P_{CO} and P_{H_2O}.

monoxide, and oxygen favors the decomposition of the hydroxycarbonyl group, serving as a hydride acceptor:

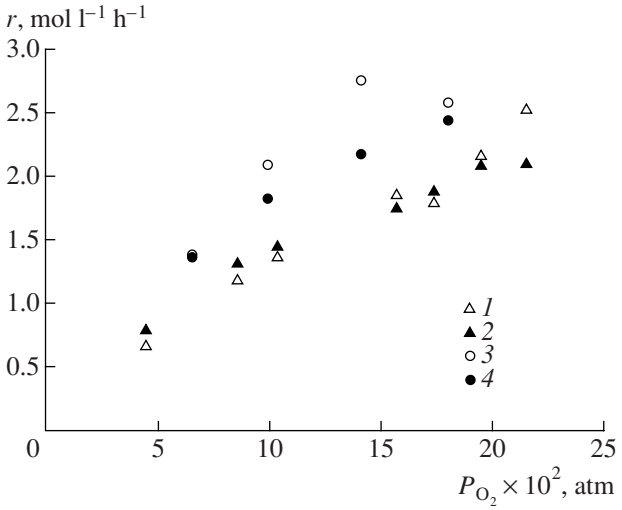

Fig. 11. (*1*, *3*) Observed and (*2*, *4*) calculated dependences of the carbon dioxide formation rate on the oxygen partial pressure at φ = (*1*, *2*) 6 and (*3*, *4*) 10 g/m^3 (calculation using Eq. (4)).

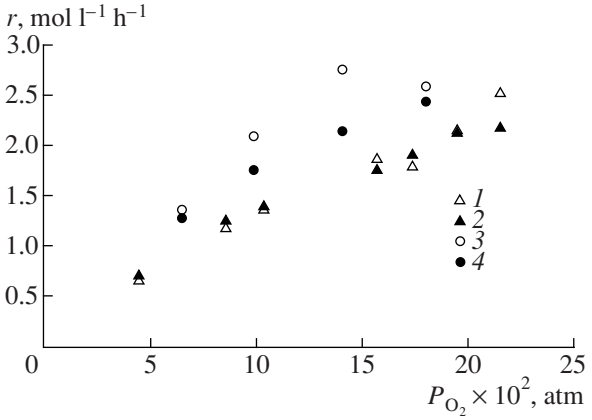

Fig. 13. (*1*, *3*) Observed and (*2*, *4*) calculated dependences of the carbon dioxide formation rate on the oxygen partial pressure at φ = (*1*, *2*) 6 and (*3*, *4*) 10 g/m^3 (calculation using Eq. (5)).

$$(1)\ \text{–PdX} + \text{CO} \overset{K_1}{\rightleftharpoons} \text{(CO)PdX},$$

$$(2)\ \text{(CO)PdX} + \text{H}_2\text{O} \overset{K_2}{\rightleftharpoons} \text{(CO)Pd(OH)} + \text{HX},$$

$$(3)\ \text{(CO)Pd(OH)} + \text{O}_2 \overset{K_3}{\rightleftharpoons} \text{(O}_2\text{)Pd(CO)(OH)},$$

$$(4)\ \text{(O}_2\text{)Pd(CO)(OH)} \overset{K_4}{\rightleftharpoons} \text{(O}_2\text{)Pd(COOH)}, \quad \text{(IX)}$$

$$(5)\ \text{(O}_2\text{)Pd(COOH)} \longrightarrow \text{CO}_2 + \text{–PdOOH},$$

$$(6)\ \text{–PdOOH} + \text{HX} \longrightarrow \text{–PdX} + \text{H}_2\text{O}_2,$$

$$(7)\ 2\text{H}_2\text{O}_2 \longrightarrow 2\text{H}_2\text{O} + \text{O}_2.$$

Equation (6), which follows from the above-mentioned chain mechanism, fit experimental data worse than mechanisms (V)–(VIII) (Table 2).

$$r = \frac{k_1 P_{CO} P_{O_2} P_{H_2O} (k_2 P_{CO} + 1)}{P_{O_2} + k_3 P_{H_2O} + k_4 P_{O_2} P_{H_2O} + k_5 P_{CO} P_{H_2O} + k_6 P_{CO} P_{O_2} P_{H_2O} + k_7 P_{CO}^2 P_{H_2O}}. \quad (6)$$

Thus, our kinetic data do not allow strict discrimination among the above hypotheses. However, the group C mechanism (VIII), which implies Eq. (5), seems to be the most likely (Figs. 12, 13).

The studies reported here demonstrated that adequate models can be based on two types of mechanisms differing in terms of the roles of water and oxygen (groups A and C).

In order to refine the mechanism, it is necessary to elucidate the source of the oxygen appearing in the resulting CO_2 and the states of copper and palladium in the active site of the catalyst. The literature concerning this point is contradictory (see above). Oxygen adsorption on Pd(II)- and Cu(II)-containing sites is unlikely. It would be very helpful to determine the kinetic isotope effects arising from the replacement of H_2O with D_2O and of $^{16}O_2$ with $^{18}O_2$. In our forthcoming studies, we will apply these approaches to the mechanistic investigation of CO oxidation, a reaction of both fundamental and practical significance.

REFERENCES

1. Markov, V.D. and Fasman, A.B., *Zh. Fiz. Khim.*, 1966, vol. 40, p. 1564.
2. Temkin, O.N., Kaliya, O.L., Zhir-Lebed, L.N., et al., *Gomogennoe okislenie* (Homogeneous Oxidation), Alma-Ata: Nauka, 1978.
3. Golodets, G.I., *Geterogenno-kataliticheskie reaktsii s uchastiem molekulyarnogo kisloroda* (Heterogeneous Catalytic Reactions Involving Molecular Oxygen), Kiev: Naukova Dumka, 1977.
4. Kuznetsova, L.I., Matveev, K.I., and Zhizhina, E.G., *Kinet. Katal.*, 1985, vol. 26, no. 5, p. 1029.
5. Rakitskaya, T.L., Ennan, A.A., and Paina, V.L., *Kataliza-tory nizkotemperaturnogo okisleniya monooksida ugle-roda* (Catalysts for Low-Temperature Carbon Monoxide Oxidation), Moscow: TsINTIKhIMNEFTEMASh, 1991.
6. Abdullaeva, A.S., *Cand. Sci. (Chem.) Dissertation*, Moscow: Lomonosov State Academy of Fine Chemical Technology, 2005.
7. Rakitskaya, T.L., Paina, V.Ya., and Ennan, A.A., *Izv. Vyssh. Uchebn. Zaved., Khim. Khim. Tekhnol.*, 1978, vol. 21, no. 7, p. 1007.
8. Rakitskaya, T.L., Paina, V.Ya., and Ennan, A.A., *Koord. Khim.*, 1987, vol. 13, no. 10, p. 1393.
9. Rakitskaya, T.L. and Paina, V.Ya., *Kinet. Katal.*, 1990, vol. 31, no. 2, p. 371.
10. Desai, M.N., Butt, J.B., and Dranoff, J.S., *J. Catal.*, 1983, vol. 79, no. 1, p. 95.
11. Choi, K.I. and Vannice, A., *J. Catal.*, 1991, vol. 127, no. 2, p. 465.
12. Choi, K.I. and Vannice, A., *J. Catal.*, 1991, vol. 127, no. 2, p. 489.
13. Choi, K.I. and Vannice, A., *J. Catal.*, 1991, vol. 131, no. 1, p. 1.
14. Jamamoto, J., Matsuzaki, T., Oxdan, K., and Okamoto, J., *J. Catal.*, 1996, vol. 161, no. 2, p. 577.
15. Lee, J.S., Choi, S.H., Kim, K.D., and Nomura, M., *Appl. Catal., B*, 1996, vol. 7, p. 199.
16. Park, E.D. and Lee, J.S., *J. Catal.*, 1998, vol. 180, no. 1, p. 123.
17. Park, E.D. and Lee, J.S., *J. Catal.*, 2000, vol. 193, no. 1, p. 5.
18. Moiseev, I.I., *π-Kompleksy v zhidkofaznom okislenii ole-finov* (π-Complexes in Liquid-Phase Alkene Oxidation), Moscow: Nauka, 1970.
19. Pavlova, S.N., Sadykov, V.A., Bulgakov, N.N., and Bredikhin, M.N., *J. Catal.*, 1996, vol. 161, no. 2, p. 517.
20. Vorontsov, A.V., Kasatkina, L.A., Dzisyak, A.P., and Tikhonova, S.V., *Kinet. Katal.*, 1979, vol. 20, no. 5, p. 1194.
21. Zudin, V.N., Likholobov, V.A., and Ermakov, Yu.I., *Kinet. Katal.*, 1977, vol. 18, no. 4, p. 921.
22. US Patent 3849336, 1974.
23. US Patent 3790662, 1974.